CD146 expression on primary nonhematopoietic bone marrow stem cells is correlated with in situ localization

Tormin, Ariane; Li, Ou; Brune, Jan Claas; Walsh, Stuart; Schütz, Birgit; Ehinger, Mats; Ditzel, Nicholas; Kassem, Moustapha; Scheding, Stefan

Published in:
Blood

DOI:
10.1182/blood-2010-08-304287

2011

CD146 expression on primary nonhematopoietic bone marrow stem cells is correlated with in situ localization

Ariane Tormin,[1] *Ou Li,[1] *Jan Claas Brune,[1] Stuart Walsh,[1] Birgit Schütz,[1] Mats Ehinger,[2] Nicholas Ditzel,[3] Moustapha Kassem,[3,4] and Stefan Scheding[1,5]

[1]Lund Stem Cell Center, University of Lund, Lund, Sweden; [2]Department of Pathology, University Hospital Lund, Lund, Sweden; [3]Molecular Endocrinology Laboratory (KMEB), Department of Endocrinology, Odense University Hospital and Medical Biotechnology Centre, University of Southern Denmark, Odense, Denmark; [4]Stem Cell Unit, College of Medicine, King Saud University, Riyadh, Saudi Arabia; and [5]Department of Hematology, University Hospital Lund, Lund, Sweden

Nonhematopoietic bone marrow mesenchymal stem cells (BM-MSCs) are of central importance for bone marrow stroma and the hematopoietic environment. However, the exact phenotype and anatomical distribution of specified MSC populations in the marrow are unknown. We characterized the phenotype of primary human BM-MSCs and found that all assayable colony-forming units-fibroblast (CFU-Fs) were highly and exclusively enriched not only in the lin$^-$/CD271$^+$/CD45$^-$/CD146$^+$ stem-cell fraction, but also in lin$^-$/CD271$^+$/CD45$^-$/CD146$^{-/low}$ cells. Both populations, regardless of CD146 expression, shared a similar phenotype and genotype, gave rise to typical cultured stromal cells, and formed bone and hematopoietic stroma in vivo. Interestingly, CD146 was up-regulated in normoxia and down-regulated in hypoxia. This was correlated with in situ localization differences, with CD146 coexpressing reticular cells located in perivascular regions, whereas bone-lining MSCs expressed CD271 alone. In both regions, CD34$^+$ hematopoietic stem/progenitor cells were located in close proximity to MSCs. These novel findings show that the expression of CD146 differentiates between perivascular versus endosteal localization of nonhematopoietic BM-MSC populations, which may be useful for the study of the hematopoietic environment. (*Blood*. 2011; 117(19):5067-5077)

Introduction

Human bone marrow contains a rare population of nonhematopoietic mesenchymal stem cells (BM-MSCs), which are multipotent and can differentiate in vivo toward skeletal lineages such as osteoblasts, adipocytes, and chondrocytes, as well as toward fibroblastic stromal cells.[1-3] In vitro, clonogenic cells—denoted as colony-forming units, fibroblast (CFU-Fs)—can be assayed from the bone marrow as plastic adherent cells giving rise to fibroblastic colonies. These CFU-Fs are considered to reflect primary BM-MSCs, and on further proliferation in culture, their descendants make up the well-known and extensively studied cultured mesenchymal stromal cells.[4]

Bone marrow CFU-Fs express surface markers such as STRO-1,[5] CD271 (nerve growth factor receptor [NGFR]),[6,7] stage-specific embryonic antigen-4 (SSEA-4),[8] GD2 (disialoganglioside 2),[9] CD49a (integrin α-1),[10] and CD146 (melanoma cell adhesion molecule [MCAM]).[3,11] To date, these different CFU-F markers have not been used in combination, and it is therefore not known whether they identify the same cells or whether different subtypes of early nonhematopoietic stem and progenitor cells coexist in the bone marrow.

Culture-expanded CD146$^+$ cells have been demonstrated to reestablish the hematopoietic microenvironment (HME) in a xenotransplantation model, and the transplanted cells colocalized with suggested HSC niches in the bone marrow.[3] Therefore, BM-MSCs are likely to be relevant for human HME and stem cell niche anatomy and function. However, a precise phenotypic definition of the human stem cell niche cellular components has thus far been elusive, in contrast to the murine system, in which different niche cell types have been recently described.[12-15]

We report herein that nonhematopoietic human BM-CFU-Fs are highly and exclusively enriched in lin$^-$/CD271$^+$/CD45$^-$/CD146$^+$ cells and in lin$^-$/CD271$^+$/CD45$^-$/CD146$^{-/low}$ cells. Whereas CD271 expression identifies all assayable BM-CFU-Fs, different expression patterns of CD146 are correlated with in situ localization differences: subendothelial sinusoidal CFU-Fs display the primary CD271$^+$/CD146$^+$ phenotype, whereas bone-lining CD271$^+$ CFU-Fs are predominantly CD146$^{-/low}$. In both locations, CD34$^+$ hematopoietic stem/progenitor cells are located in close proximity, which might enable for the first time the prospective investigation and dissection of differently localized putative HSC niche cells in human bone marrow.

Methods

BM-MNCs

Sixty milliliters of bone marrow was aspirated from the iliac crest bone of consenting healthy donors. This procedure was approved by the University of Lund ethics committee. Bone marrow mononuclear cells (BM-MNCs)

Submitted August 30, 2010; accepted March 6, 2011. Prepublished online as *Blood* First Edition paper, March 17, 2011; DOI 10.1182/blood-2010-08-304287.

*O.L. and J.C.B. contributed equally to this study.

The online version of this article contains a data supplement.

The publication costs of this article were defrayed in part by page charge payment. Therefore, and solely to indicate this fact, this article is hereby marked "advertisement" in accordance with 18 USC section 1734.

were isolated by density gradient centrifugation using LSM 1077 Lymphocyte Separation Medium (PAA Laboratories) either with or without prior incubation with RosetteSep Human Mesenchymal Stem Cell Enrichment Cocktail (StemCell Technologies) for lineage depletion (CD3, CD14, CD19, CD38, CD66b, and glycophorin A).

FACS

Lineage-depleted BM-MNCs were incubated in blocking buffer (Dulbecco PBS [DPBS] without Ca^{2+}, Mg^{2+}, and 3.3 mg/mL of human normal immunoglobulin [Gammanorm; Octapharm] and 1% FBS [Invitrogen]) to prevent unspecific binding, followed by staining with monoclonal antibodies against CD45, CD146, and CD271 (see supplemental Methods, available on the *Blood* Web site; see the Supplemental Materials link at the top of the online article). Sorting gates were set according to the corresponding fluorescence-minus-one (FMO) controls. Cells were sorted on a FACSAria I or a FACSDiva flow cytometer (both BD Biosciences). Dead cells were excluded by 7-amino-actinomycin (7-AAD; Sigma) staining, and doublets were excluded by gating on forward scatter-height versus forward scatter-width and side scatter-height versus side scatter-width.

Generation of cultured mesenchymal stromal cells

Sorted BM-MNCs were cultured in standard MSC culture medium (NH Expansion Medium [Miltenyi Biotec] plus 1% antibiotic-antimycotic solution [Sigma-Aldrich]). Medium was changed weekly and cells were passaged at 70% confluence after trypsinization (0.05% trypsin/EDTA; Invitrogen). Trypsinized cells were replated at 500-1000 cells/cm^2.

Mesenchymal stromal cells for intra-bone marrow transplantation or subcutaneous transplantation with hydroxyapatite/tricalcium phosphate (HA/TCP) carriers were initiated from sorted $CD271^+/CD45^-/CD146^{-/low}$ and $CD271^+/CD45^-/CD146^+$ BM-MNCs, respectively. Sorted cells were initially plated at 20-50 cells/cm^2, and adherent cells were culture expanded as described in the beginning of this section. Green fluorescent protein (GFP)–labeled cells for intra-bone marrow transplantation were produced by transducing 0. passage cells (before the first passaging) with a lentiviral vesicular stomatitis virus glycoprotein GFP vector, followed by sorting of GFP^+ cells 2 weeks after transduction and an additional 3 weeks of culture until transplantation.

CFU-F assay

CFU-F frequencies of BM-MNC populations were determined as described previously.[16,17] Briefly, FACS-sorted cells were cultured at plating densities of 1-50 cells/cm^2 when assaying $CD271^+/CD45^-/CD146^{-/low}$ and $CD271^+/CD45^-/CD146^+$ sorted cells and at 5000 cells/cm^2 for sorting viable and $CD45^+$ cells. Colonies were counted after 14 days (1% crystal violet; Sigma-Aldrich). Generally, assays were set up in duplicates or triplicates.

For single-cell CFU-F assays, cells were sorted into fibronectin-coated, 96-well plates and cultured in MSC medium. Single-cell–derived colonies were counted after 3 weeks, harvested by trypsinization, and split for continued culture for in vitro differentiation and FACS analysis, respectively.

Hematopoietic progenitor and LTC-IC assays

For long-term culture-initiating cell (LTC-IC) assays, CD271/CD45 populations were sorted from MACS-enriched primary $CD271^+$ BM-MNCs (CD271 MicroBead kit; Miltenyi Biotec). Cells were resuspended in IMDM plus 2% FBS (both Invitrogen) and seeded into methylcellulose medium (HSC-CFU complete with Epo; Miltenyi Biotec). After 2 weeks of culture, hematopoietic colonies were analyzed under a microscope according to standard criteria.

The stroma-supporting capacities of cultures generated from sorted $CD271^+/CD45^-/CD146^{-/low}$ and $CD271^+/CD45^-/CD146^+$ cells were assessed with standard LTC-IC assays. Briefly, 3×10^5 cells were plated in collagen-coated, 35-mm culture dishes and irradiated the following day (16 Gy). Forty-eight hours after irradiation, 3000 MACS-enriched human cord blood $CD34^+$ cells were seeded and cultured in MyeloCult H5100 medium (StemCell Technologies) with 10^{-3}mM hydrocortisone (Sigma-Aldrich) with weekly half-medium changes. After 6 weeks, cells were harvested by trypsinization and assayed for hematopoietic colony formation, as described in the beginning of this section.

Flow cytometry

Cultured cells were harvested (0.05% trypsin/EDTA) and washed, and unspecific binding was blocked with human normal immunoglobulin. Cells were stained for 45 minutes at 4°C with combinations of antibodies. Samples were analyzed on a FACSCalibur flow cytometer (BD Biosciences).

Freshly isolated, RosetteSep-depleted BM-MNCs were stained with a combination of antibodies, including CD271, CD146, and CD45. Analysis was performed on an LSR II flow cytometer (BD Biosciences). For antibodies and suppliers, see supplemental Methods. Dead cells were excluded by 7-AAD staining. For all samples analyzed on the LSR II, doublets were excluded. Intracellular staining for nestin was performed on fixed and permeabilized cells (Cytofix/Cytoperm Kit; BD Biosciences) using FITC-conjugated anti–human-nestin antibody and the corresponding isotype control (both R&D Systems).

In vitro differentiation assays

Cultured BM mesenchymal stromal cells were differentiated toward the adipogenic, osteoblastic, and chondrogenic lineage, as described previously.[16,17] Briefly, cells were cultured for 14 days in AdipoDiff medium (Miltenyi Biotec), and cells were stained with Oil Red O (Sigma-Aldrich). For osteogenic differentiation, cells were cultured in osteogenesis induction medium (standard MSC medium supplemented with 0.05mM ascorbic acid [Wako Chemicals] and 0.1μM dexamethasone and 10mM β-glycerophosphate [both from Sigma-Aldrich]) for 21 days, and calcium depositions in the cultures were detected with Alizarin Red (Sigma-Aldrich). Chondrogenic differentiation was accomplished by culturing cell pellets (2.5×10^5 cells/pellet) for 28 days in chondrogenesis induction medium (DMEM high-glucose medium supplemented with 0.1μM dexamethasone, 1mM sodium pyruvate, and 0.35mM L-proline [all from Sigma-Aldrich], 0.17mM ascorbic acid [Wako Chemicals], 1% ITS plus (insulin transferrin selerium) culture supplements [BD Biosciences], and 0.01 μg/mL of TGF-β3 [R&D Systems]). Pellets were paraformaldehyde fixed and frozen in O.C.T. Compound (Sakura). Cryosections were stained against aggrecan (see supplemental Methods) and toluidine blue and Alcian blue (both Sigma-Aldrich). For aggrecan stainings, nuclei were stained with 4′,6-diamidino-2-phenylindole (Invitrogen). Sections were analyzed with a fluorescence microscope (BX51; Olympus) and a digital camera (DP70; Olympus) using DP manager software version 1.1.1.71 (Olympus).

Single-cell multiplex PCR

For single-cell PCR, $CD271^+/CD45^-/CD146^{-/low}$ and $CD271^+/CD45^-/CD146^+$ BM-MNCs were sorted into 96-well plates (Thermo Scientific) containing 4 μL/well of lysis buffer (2.5mM dNTP [Takara Bio] plus 10% NP40, 0.1M DTT, and 40 U/mL of RNase Out [all Invitrogen]). Plates were spun, frozen, and stored at −80°C until analysis. Reverse transcription/first-strand synthesis was performed at 37°C for 60 minutes after adding Moloney murine leukemia virus–reverse transcriptase (200 U/μL) and 5× first-strand buffer (both Invitrogen) and outer reverse primers to each well. The first round of PCR was performed with 10 μL of reverse transcriptase reaction, outer forward primers, and Taq polymerase (Takara Bio) at 94°C for 1 minute, 60°C for 1 minute, and 72°C for 2 minutes for 34 cycles and then 72°C for 7 minutes. The second round of PCR was performed for each gene with 1 μL of first-round PCR product, the inner primer pair, and Taq polymerase at 94°C for 30 seconds, 60°C for 1 minute, and 72°C for 1 minute for 34 cycles and then 72°C for 7 minutes. PCR products were loaded on 2% agarose E-gels with E-Gel Low-Range DNA Ladder (both Invitrogen) and analyzed. Primer sequences are provided in supplemental Methods.

In vivo transplantation

For orthotopic transplantations, 1×10^6 GFP^+ mesenchymal stromal cells generated from sorted $CD271^+/CD45^-/CD146^{-/low}$ and $CD271^+/CD45^-/CD146^+$ BM-MNCs were injected intrafemorally into irradiated (2 Gy) 6- to 8-week-old NOD–Cg-*Prkdc*^{scid} *Il2rg*^{tm1Wjl}/SzJ mice. After 8 weeks,

mice were killed by cervical dislocation and femurs were removed and fixed in paraformaldehyde. After decalcification, permeabilization, and dehydration, specimens were embedded in paraffin for analysis.

For analysis of in vivo bone and stroma formation, cultured MSCs were derived from sorted CD271$^+$/CD45$^-$/CD146$^{-/low}$ and CD271$^+$/CD45$^-$/CD146$^+$ cells. Cells were loaded overnight on HA/TCP ceramic powder, and 4×10^5 cells were implanted subcutaneously into 8-week-old female NOD/SCID mice (4 implants per culture). Implants were removed after 8 weeks, fixed, decalcified, and paraffin embedded. Sections were stained with hematoxylin/eosin and analyzed as described previously.[18] All animal procedures were approved by the local ethical committees on animal experiments.

Immunofluorescence staining of bone sections

Paraffin sections from human bone marrow and mouse femurs were deparaffinized and rehydrated following standard protocols. Heat-induced epitope retrieval was applied using citrate buffer, pH 6 (Target Retrieval Solution; Dako) for 30 minutes at 98°C. Sections were blocked/permeabilized with Dulbecco PBS and 0.3% Triton X-100 (Sigma-Aldrich), 10% normal goat serum, 0.1% sodium azide, and 0.1% cold fish-skin gelatin (Sigma-Aldrich), and stained for 1 hour at room temperature or overnight at 4°C with primary antibodies. After washing, secondary staining was performed for 1 hour at room temperature (for antibodies, see supplemental Methods). TO-PRO-3 (Invitrogen) was used as a nuclear stain. Photographs were taken on a confocal microscope (DMRE; Leica) equipped with green helium/neon, standard helium/neon, and argon lasers using Confocal Software v2.61 (Leica).

Hypoxia experiments

Stromal cultures generated from unfractionated bone marrow were cultured with the addition of 100μM deferoxamine mesylate in a standard incubator with daily medium changes. After 1 week, cells were analyzed by FACS for the expression of CD146 and other surface markers.

Cultures generated from unfractionated bone marrow were cultured in a hypoxic chamber set to 1% O_2 in standard MSC medium with weekly medium changes. After 2 weeks, cells were analyzed by FACS for the expression of CD146 and other surface markers (see supplemental Methods).

Results

CFU-Fs are highly and exclusively enriched in CD271$^+$/CD45$^-$ BM-MNCs expressing either CD146$^{-/low}$ or CD146$^+$

Human BM-MNCs were stained with antibodies against CD146, CD271, and CD45 (Figure 1A-B). Without CD45 exclusion, CD271/CD146 populations contained large numbers of hematopoietic cells, (43%, 97%, and 88% of CD271$^+$/CD146$^+$, CD271$^+$/CD146$^-$, and CD271$^-$/CD146$^+$ cells, respectively; n = 9). As shown in Figure 1C, we detected 0.02% ± 0.005% CD271$^+$/CD45$^-$/CD146$^+$, 0.01% ± 0.003% CD271$^+$/CD45$^-$/CD146$^-$, and 0.06% ± 0.02% CD271$^-$/CD45$^-$/CD146$^+$ cells within viable human BM-MNCs (data are mean ± SEM; n = 9).

We next assessed the CFU-F frequency of the different CD271/CD146 cell populations in lineage-depleted bone marrow (Figure 1D-G). CFU-Fs were highly and exclusively enriched in the CD271$^+$/CD45$^-$/CD146$^{-/low}$ and CD271$^+$/CD45$^-$/CD146$^+$ cells. In contrast, colony growth was not observed in either CD45$^+$ or the CD271$^-$ cell fractions regardless of CD146 expression (Figure 1F). No CFU-Fs were lost by lineage depletion (supplemental Figure 1)

Mean CFU-F frequencies were 4.2 ± 1.6 CFU-Fs per 100 plated CD271$^+$/CD45$^-$/CD146$^{-/low}$ cells and 2.0 ± 0.7 CFU-Fs per 100 CD271$^+$/CD45$^-$/CD146$^+$ cells compared with 0.005 ± 0.001 CFU-Fs per 100 viable cells in lineage-depleted BM-MNCs (Figure 1F).

The colony-forming potential of the 2 CFU-F–containing populations was confirmed by single-cell assays. CFU-F frequencies were 3.5 ± 0.9 and 1.6 ± 0.7 per 96-well plate for CD271$^+$/CD45$^-$/CD146$^{-/low}$ and CD271$^+$/CD45$^-$/CD146$^+$ cells, respectively (n = 8; Figure 1G). Single-cell sorting accuracy as estimated by bead sorting was 100%.

Whereas CD146 expression on CD271$^+$ cells did not discriminate between colony-forming and non–colony-forming cells, CD45 expression did; the majority of CD271$^+$ cells coexpressed CD45, and clear morphologic differences were observed between the CD271$^+$/CD45$^-$ and CD271$^+$/CD45$^+$ cell populations (supplemental Figure 2B).

In addition to CFU-F potential, sorted bone marrow cell populations were also tested for hematopoietic colony growth in standard methylcellulose assays. Erythroid colonies were observed at low frequencies when CD271$^+$/CD45$^+$ cells were plated, but were absent in other sorted cell fractions (supplemental Figure 2).

Both CD271$^+$/CD45$^-$/CD146$^{-/low}$ and CD271$^+$/CD45$^-$/CD146$^+$ BM-MNCs give rise to typical cultured mesenchymal stromal cells

We generated mesenchymal stromal cell cultures from both CD271$^+$/CD45$^-$/CD146$^{-/low}$ and CD271$^+$/CD45$^-$/CD146$^+$ cells derived from either bulk- or single-sorted cells. Both populations grew in standard MSC medium as typical adherent, spindle-shaped, fibroblastic-like cells (Figure 2A), and no significant differences in colony size between CD146$^+$ cells (2.1 ± 0.1 mm; n = 46) and CD146$^{-/low}$ cells (1.9 ± 0.08 mm; n = 51) could be observed (Figure 2B). In addition, cultured cells from both populations exhibited similar differentiation potential in vitro toward the osteoblastic (Alizarin Red staining; some clones were additionally stained with von Kossa/ALP), adipogenic (Oil Red O staining), and chondrogenic (aggrecan, toluidine blue, and Alcian blue staining) lineages. This was observed for both single-cell–derived clonal cultures (Figure 2C) and multiclonal cultures from bulk-sorted cells. A sufficient number of cells to test for trilineage differentiation were generated from 14 of 20 clones, 8 of which showed differentiation into all 3 lineages (2 of 3 CD146$^+$ clones and 6 of 11 CD146$^{-/low}$ clones). The remaining 6 clones showed either 2-lineage differentiation capacity (n = 3) or only unilineage differentiation capacity (n = 3). Sufficient cells for testing bilineage differentiation capacity (osteoblasts and adipocytes) could be generated from 2 additional clones, 1 of which showed bilineage capacity and the other unilineage capacity for osteoblastic differentiation. Furthermore, 2 additional clones could be only tested for osteoblastic differentiation and both of them were positive. In general, bilineage or unilineage clones possessed osteoblastic potential but lacked or lost adipogenic and/or chondrogenic potential. Furthermore, stromal cell cultures generated from CD271$^+$/CD45$^-$/CD146$^{-/low}$ and CD271$^+$/CD45$^-$/CD146$^+$ CFU-Fs (single-cell as well as bulk) exhibited similar surface-marker profiles when analyzed for expression of typical MSC marker profiles (ie, cells were positive for CD105, CD90, CD73, and HLA-class I, and negative for CD34, CD45, CD14, CD19, and HLA-DR; Figure 2D and supplemental Figure 3). Moreover, cultures derived from CD271$^+$/CD45$^-$/CD146$^{-/low}$ and CD271$^+$/CD45$^-$/CD146$^+$ cells showed no differences in stroma-supporting capacity, as indicated by standard LTC-IC assays (21.0 ± 3.0 vs 20.7 ± 3.5 colonies per 1000 seeded CD34$^+$ cells; n = 3).

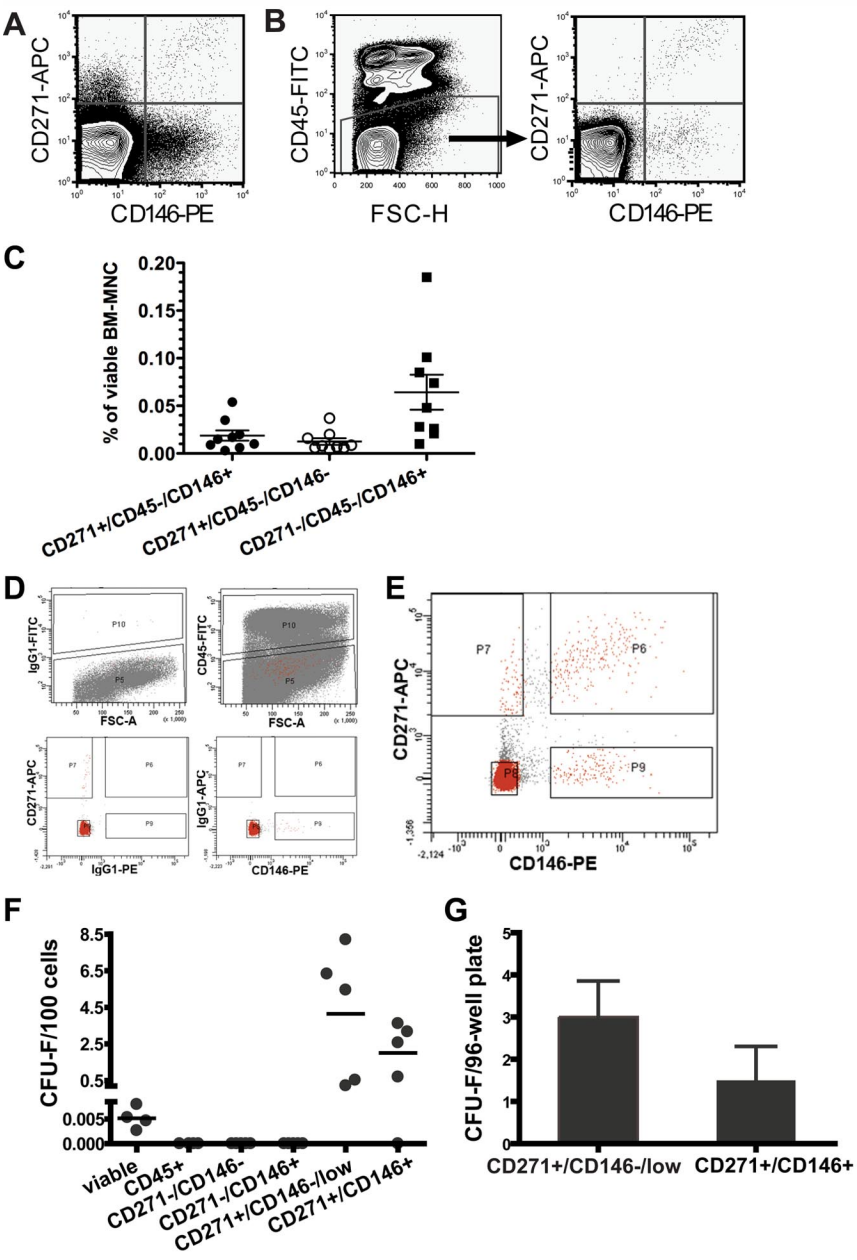

Figure 1. All CFU-Fs in human bone marrow are contained in the CD271$^+$/CD45$^-$/CD146$^{-/low}$ and the CD271$^+$/CD45$^-$/CD146$^+$ fraction. Freshly isolated human BM-MNCs were stained with antibodies against CD271, CD146, and CD45, and analyzed by flow cytometry. Representative contour plots of CD271- and CD146-expressing human bone marrow cells after forward/side scatter and 7-AAD gating are shown. (A) CD271 and CD146 expression in whole viable BM-MNCs. (B) CD271 and CD146 expression after exclusion of CD45$^+$ cells. (C) Percentage of CD271$^+$/CD45$^-$/CD146$^+$, CD271$^+$/CD45$^-$/CD146$^-$, and CD271$^-$/CD45$^-$/CD146$^+$ cells in viable, nondepleted human BM-MNCs (n = 9). Horizontal lines indicate mean values. Error bars show SEM. (D) Gates for the CD271/CD45/CD146 sorts from lineage-depleted bone marrow were set according to the appropriate FMO controls for CD45 (top row left plot). The top right plot illustrates the CD45-sorting gate, with P10 and P5 indicating the sorting gates for CD45$^+$ cells and CD45$^-$ cells, respectively. Red dots indicate all gated events shown in the CD271/CD146 plot (E) after backgating on CD45. Sorting gate definition based on the FMO controls for CD271 and CD146 are illustrated in the bottom plots. (E) Sorting gates from a representative bone marrow sample for CD271$^-$/CD146$^-$ (P8), CD271$^-$/CD146$^+$ (P9), CD271$^+$/CD146$^{-/low}$ (P7), and CD271$^+$/CD146$^+$ (P6) after lineage depletion and CD45 exclusion. As shown in this analysis, CD146 expression increased gradually with increasing CD271 expression, and therefore it is impossible to identify a clear-cut CD271$^+$/CD146$^-$ cell population within the CD271$^+$ cells. We therefore chose instead to use the term CD271$^+$/CD146$^{-/low}$ for cells sorted on gate P7 to indicate this fact. (F) CFU-F frequencies per 100 freshly isolated BM-MNCs of total viable cells sorted only based on 7-AAD exclusion (viable, n = 4), sorted total CD45$^+$ cells (n = 4), and the different sorted CD271/CD146 populations after CD45 exclusion (n = 5). Each dot represents the mean frequency of CFU-Fs from one bone marrow sample. Horizontal lines indicate mean values of at least 4-5 independent samples. (G) CFU-F frequencies per 96-well plate of single-sorted CD271$^+$/CD45$^-$/CD146$^{-/low}$ and CD271$^+$/CD45$^-$/CD146$^+$ primary cells. Data are shown as mean ± SEM (n = 8).

Primary CD271$^+$/CD146$^{-/low}$ and CD271$^+$/CD146$^+$ CFU-Fs share a similar phenotype

We compared the uncultured CD271$^+$/CD45$^-$/CD146$^{-/low}$ and CD271$^+$/CD45$^-$/CD146$^+$ CFU-F–containing populations based on morphology, FACS profile, and gene expression. As shown in Figure 3, freshly sorted cells before attachment were round and displayed reticular extensions (Figure 3A-B left). After attachment, cells displayed a large, flat, branched-out fibroblastic morphology (Figure 3A-B right). In addition, cytospin preparations were prepared to study nuclear morphology and cytoplasm properties of freshly isolated cells in more detail (supplemental Figure 4A-C). CD271$^+$/CD45$^-$/CD146$^{-/low}$ and CD271$^+$/CD45$^-$/CD146$^+$ cells were characterized by cytoplasmic vacuoles and large, immature nuclei with an open chromatin pattern, and CD271$^+$/CD146$^{-/low}$ cells were generally smaller than the double-positive cells (supplemental Figure 4A-B). In contrast, CD146 single-positive cells, which did not contain any CFU-Fs, also had immature nuclei but exhibited a more basophilic cytoplasm and perinuclear halos, which clearly distinguished them from CD271-positive CFU-Fs (supplemental Figure 4C). We also investigated sorted primary CD271$^+$/CD45$^+$ BM-MNCs, which displayed clear morphologic differences compared with the CFU-F–containing CD271$^+$/CD45$^-$ cell population (supplemental Figure 2B).

Multicolor FACS analysis of lineage-depleted BM-MNCs (n = 4) was performed to assess the coexpression of signature mesenchymal and stromal cell-surface marker profiles on CD271$^+$/CD45$^-$/CD146$^{-/low}$ and CD271$^+$/CD45$^-$/CD146$^+$ cells. As illustrated in Figure 3C, primary cells from both CFU-F populations showed coexpression of CD105, CD90, and STRO-1, as well as PDGFR-beta. The majority of the cells, however, failed to express SSEA-4 and GD2. However, CD271$^+$/CD45$^-$ cells coexpressed integrin α 1 (CD49a) (supplemental Figure 4D) and nestin (supplemental Figure 4E). Endothelial markers such as

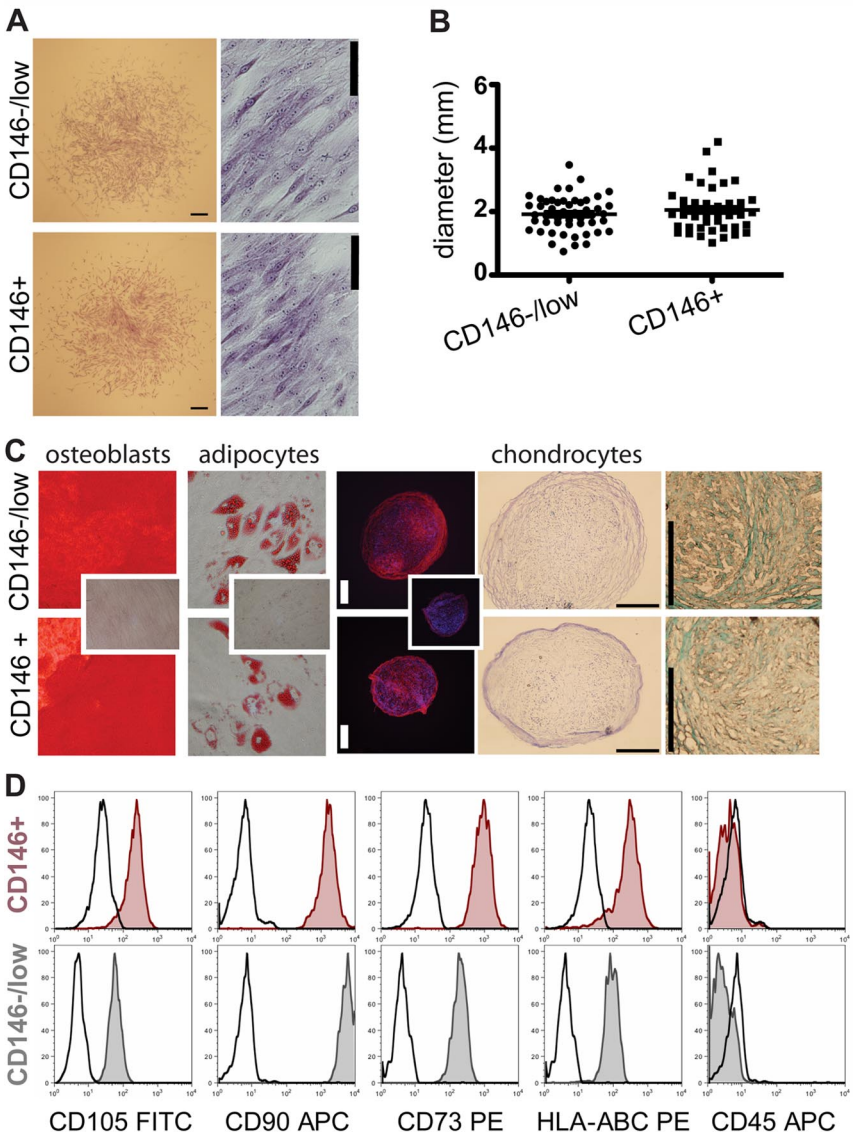

Figure 2. Cultured CD271$^+$/CD45$^-$/CD146$^{-/low}$ and CD271$^+$/CD45$^-$/CD146$^+$ BM-MNCs give rise to standard mesenchymal stromal cell cultures. Morphology, differentiation capacity, and FACS profile of cultured CD271$^+$/CD45$^-$/CD146$^{-/low}$ and CD271$^+$/CD45$^-$/CD146$^+$ cells were compared. (A) Fibroblastic colonies derived from CD146$^{-/low}$ cells and CD146$^+$ cells on day 14 shown with crystal violet staining. Scale bars for the colonies indicate 400 μm; scale bars for the close-ups indicate 50 μm. (B) Mean diameter of CD271$^+$/CD45$^-$/CD146$^+$- and CD271$^+$/CD45$^-$/CD146$^{-/low}$-initiated colonies (day 14). Every dot represents one colony (CD146$^+$ n = 46; CD146$^{-/low}$ n = 51) of 2 independent experiments. The lines represent the mean diameter of the colonies in millimeters. Error bars represent SEM. (C) In vitro differentiation capacity of cultures generated from a single CD271$^+$/CD45$^-$/CD146$^{-/low}$–sorted cell (top row) and a single CD271$^+$/CD45$^-$/CD146$^+$–sorted cell (bottom row) from the same bone marrow sample. Clonal cultures were differentiated toward the osteoblastic, adipogenic, and chondrogenic lineage. Osteoblasts were stained with Alizarin Red (left), and adipocytes were stained with Oil Red O (second from left). Small inserted photographs show Alizarin Red and Oil Red O staining on undifferentiated cells. Original magnifications were 40× and 200×, respectively. Chondrocyte pellets were stained with an anti-aggrecan plus secondary antibody (third from right). Control sections were stained with the secondary antibody only (small inserted photograph). In addition, chondrocyte sections were stained with toluidine blue (second from right) for proteoglycans and Alcian blue (far right) for metachromasia. Scale bars indicate 200 μm. (D) Representative FACS profile of single-cell–derived cultured stromal cells. Cells were measured in the fourth and second passages, when sufficient amounts were available. Cultures were initiated with either a CD271$^+$/CD45$^-$/CD146$^+$ (red tinted histograms) or a CD271$^+$/CD45$^-$/CD146$^{-/low}$ (gray tinted histograms) FACS-sorted bone marrow cell. Cultured cells were stained for typical MSC markers and analyzed by flow cytometry. Black open histograms represent the corresponding isotype controls.

CD31 and CD34 were only expressed on CD146 single-positive (ie, non-CFU-F–containing) cells (Figure 3C).

Multiplex single-cell PCR of sorted, uncultured CD271$^+$/CD45$^-$/CD146$^{-/low}$ cells (Figure 3D) and CD271$^+$/CD45$^-$/CD146$^+$ cells (Figure 3E) were performed. Tissue-nonspecific alkaline phosphatase was expressed by virtually all CD271$^+$/CD45$^-$/CD146$^{-/low}$ and CD271$^+$/CD45$^-$/CD146$^+$ cells. Genes involved in adipogenic differentiation (eg, CEBPA and LPIN1) also exhibited a similar expression in both CFU-F populations. Further, both populations expressed genes such as Nanog, Oct-4, and Sox2 (for protein expression, see supplemental Figure 4F). Interestingly, CD146 expression could also be detected in approximately 40% of the CD271$^+$/CD45$^-$/CD146$^{-/low}$ cells; however, the band intensity was weaker compared with CD271$^+$/CD45$^-$/CD146$^+$ cells, thus matching the flow cytometric profile of a gradually increasing CD146 expression (Figure 1B and 1E). CD45 expression was generally not detected.

In vivo differentiation capacity of cultured CD271$^+$/CD146$^{-/low}$ and CD271$^+$/CD146$^+$ cells

CD271$^+$/CD45$^-$/CD146$^{-/low}$ and CD271$^+$/CD45$^-$/CD146$^+$ CFU-Fs were culture expanded in standard MSC medium to obtain sufficient cell numbers for heterotopic (subcutaneous) and orthotopic (intrafemoral) transplantation into immunodeficient mice. Eight weeks after subcutaneous injection (cultured cells with HA/TCP carrier particles), bone, adipocytes, fibroblastic tissue, and capillaries could be detected in both transplants (Figure 4A). In addition, we detected invading hematopoietic cells in the transplants (Figure 4B).

Orthotopic intrafemoral transplantations into irradiated NOD–Cg-*Prkdc*^{scid} *Il2rg*^{tm1Wjl}/SzJ mice were performed with GFP-labeled stromal cultures generated from either CD271$^+$/CD45$^-$/CD146$^{-/low}$ or CD271$^+$/CD45$^-$/CD146$^+$ cells. After 8 weeks, GFP$^+$ cells could be detected in the perivascular regions surrounding the endothelium of vessels, as cells lining the surface of cortical and trabecular bone or surrounding adipocytes, or as reticular cells in the marrow space (Figure 4C-E). Some of the bone-lining GFP$^+$ cells were found to express N-cadherin (Figure 4C). The majority of transplanted GFP$^+$ cells were localized in close proximity (ie, within 20μm, corresponding to approximately 2 cells) of the bone surface and vasculature, respectively (supplemental Table 1). No differences in the distribution of transplanted CD271$^+$/CD45$^-$/CD146$^{-/low}$–derived cells were observed compared with CD271$^+$/CD45$^-$/CD146$^+$–derived cultures.

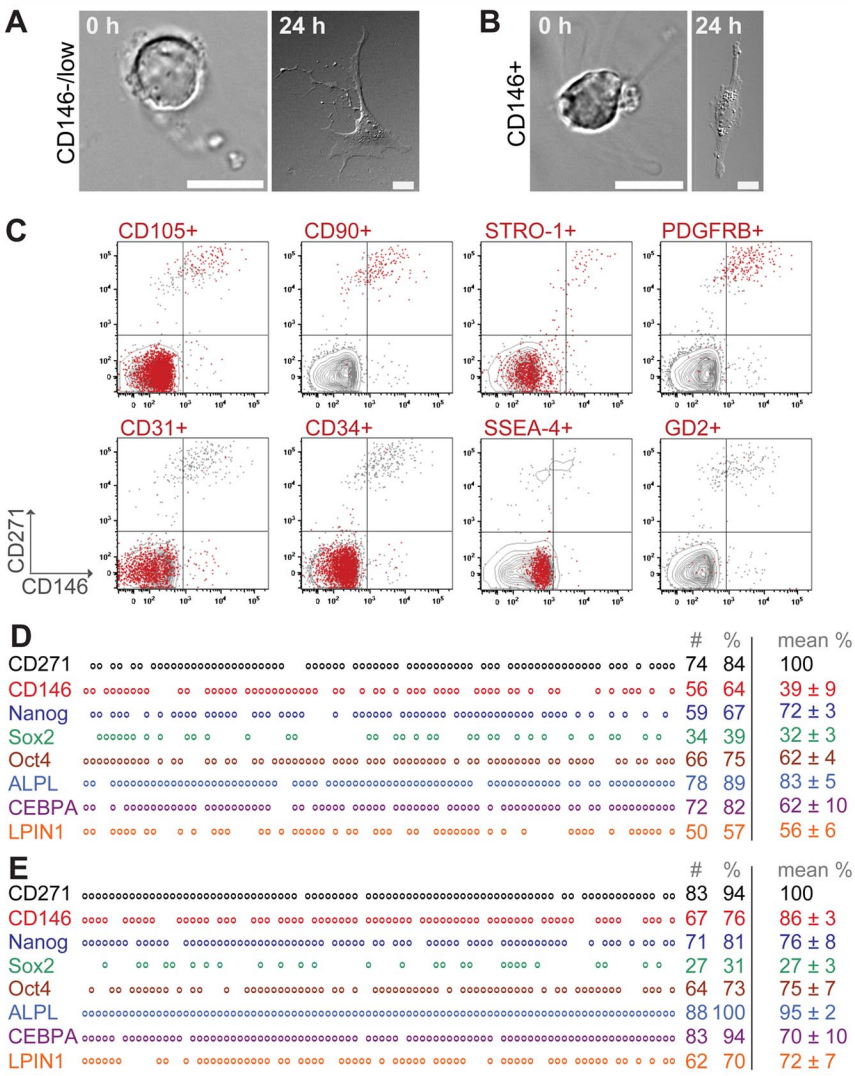

Figure 3. Morphology, surface-marker profile, and gene expression of primary CD271$^+$/CD146$^{-/low}$ and CD271$^+$/CD146$^+$ CFU-Fs. Freshly sorted cells expressing CD271$^+$/CD45$^-$/CD146$^{-/low}$ (A) and CD271$^+$/CD45$^-$/CD146$^+$ (B) were allowed to sediment (0 hours) or to adhere for 24 hours to slides. Photographs were taken on a differential interference contrast microscope (Axiovert 200M; Zeiss). Scale bars indicate 10 μm. (C) Representative multicolor FACS analysis of primary, lineage-depleted BM-MNCs after CD45 exclusion. Events are plotted for CD146 (x-axis) against CD271 (y-axis). Red events in the plots indicate cells that coexpress the marker listed on top of the plot: CD105, CD90, STRO-1, PDGFR-β, SSEA-4, GD2, CD31, and CD34. Gray events represent cells that did not coexpress the listed marker. Each plot represents an individually stained sample tube from the same bone marrow sample. The mean percentage of CD271$^+$ cells was of 0.14% ± 0.01% in all plots. (D-E) Single-cell multiplex PCR of sorted, uncultured CD271$^+$/CD45$^-$/CD146$^{-/low}$ (D) and CD271$^+$/CD45$^-$/CD146$^+$ (E) cells. Representative results from one donor are shown. Each vertical column represents a single cell and each horizontal row represents a certain analyzed gene. Circles indicate expression of the gene, whereas blanks indicate that no PCR band was detected. In total, sorted cells from 3-4 different donors were analyzed. Numbers indicate the number (#) and percentage (%) of positive cells per plate of the donor sample presented in the figure. Data in the right column represent mean percentages of positive cells of all analyzed samples. The number of CD271$^+$ wells is set as 100%. For the mean percentages, cells were only included when they showed a positive band for CD271.

The principal capacity of transplanted cells to form secondary colonies was investigated qualitatively in first experiments by harvesting bone marrow cells from 2 mice 8 weeks after intrafemoral transplantation and plating them for CFU-Fs in standard MSC culture medium. GFP$^+$ fibroblastic colonies were detected in the bone marrow of mice transplanted with CD271$^+$/CD45$^-$/CD146$^{-/low}$- or CD271$^+$/CD45$^-$/CD146$^+$–derived cells, thus demonstrating the principally colony-forming capacity of transplanted BM-MSC–derived cells. However, these experiments were not designed to allow for a quantitative analysis.

In situ localization of CD271$^+$/CD146$^{-/low}$ and CD271$^+$/CD146$^+$ cells in human bone marrow

To investigate the in situ localization of BM-CFU-Fs, paraffin sections of normal human bone marrow were stained with antibodies against CD146 and CD271. CD146/CD271 double-positive cells were observed as perivascular cells surrounding the capillary endothelium and larger vessels (Figure 5A-B and supplemental Figure 5B-E). CD271$^+$ reticular cells spanned the bone marrow with long extensions, some of which encircled adipocytes. In contrast to these CD146/CD271 double-positive cells, we found that bone-lining cells proximal to the surface of trabecular bone primarily expressed CD271 alone (Figure 5C and supplemental Figure 5A). CD146 coexpression by bone-lining cells was rarely detected. Costaining with CD45 confirmed that no perivascular, reticular, or bone-lining cells were CD45$^+$ (Figure 6A). In the marrow space, CD271^{dim}-coexpressing hematopoietic CD45$^+$ cells were visible as smaller, round cells (Figure 6A right), and these cells could easily be distinguished from CD271^{bright} reticular cells based on their morphology. CD146 was not only expressed by perivascular cells, but also by α-smooth muscle actin (α-SMA)–positive cells within the vascular tunica media (supplemental Figure 5C), whereas CD271 expression was exclusively confined to the extraluminal cells in the vascular tunica adventitia (Figure 6B and supplemental Figure 5B). CD271$^+$ and CD146$^+$ cells in the tunica adventitia exhibited weak expression of α-SMA (Figure 6B and supplemental Figure 5B-C).

We next investigated the colocalization of CD34$^+$ hematopoietic stem/progenitor cells with CFU-Fs in bone marrow sections. As illustrated in Figure 6, human, round CD34$^+$ cells could be found in proximity to perivascular cells stained with CD271 (Figure 6C). In addition, CD34$^+$ cells could be detected in proximity to trabecular bone-lining CD271$^+$ cells (Figure 6D), although, as expected, only at very low frequencies.

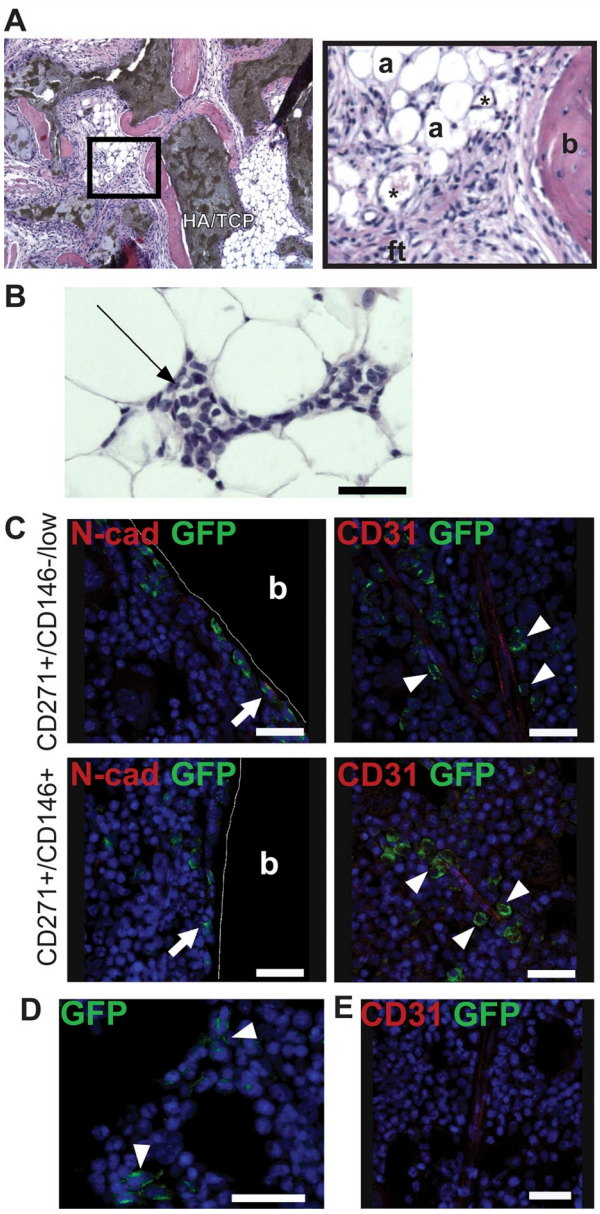

Figure 4. Ectopic and orthotopic transplantation of cultured cells into immunodeficient mice. Multiclonal cultures generated from CD271$^+$/CD45$^-$/CD146$^{-/low}$ and CD271$^+$/CD45$^-$/CD146$^+$ primary BM-MNCs were transplanted either subcutaneously (with HA/TCP particles) or intrafemorally into immunodeficient mice. (A-B) Representative section of hematoxylin/eosin–stained transplanted cells and HA/TCP carrier particles 8 weeks after subcutaneous transplantation of CD271$^+$/CD45$^-$/CD146$^+$–derived MSCs. (A) Bone (b), adipocytes (a), fibroblastic tissue (ft), and capillaries (*) are indicated. Dark brown areas in the left photograph indicate HA/TCP carrier particles. Black square in the left photograph is shown as a magnification (original magnification 10×). (B) Invading hematopoietic cells could be detected in the transplanted cells (black arrow). Original magnification was 10×. Scale bar indicates 50 μm. (C) GFP$^+$ cells generated from either CD271$^+$/CD45$^-$/CD146$^{-/low}$ (top row) or CD271$^+$/CD45$^-$/CD146$^+$ (bottom row) cells analyzed 8 weeks after intrafemoral transplantation. GFP$^+$ cells (green) could be detected as bone-lining cells, some of which expressed N-cadherin (N-Cad, red) (white arrows, left panels), and in perivascular regions surrounding the endothelium (CD31, red) (white arrowheads, right panels). (D) Reticular GFP$^+$ cells (green) could be detected independently from vessels in the marrow space (white arrowheads). The photograph shows reticular GFP$^+$ cells generated from CD271$^+$/CD45$^-$/CD146$^{-/low}$ cells. (E) Bone marrow section from a control mouse (injected with Dulbecco PBS only) stained with anti–GFP and CD31 antibody. Nuclei were stained with TO-PRO3 (blue). Cortical bone (b) is indicated. Scale bars indicate 25 μm. The photographs were taken with a confocal microscope (DMRE; Leica).

In vitro CD146 expression is up-regulated during culture and down-regulated under hypoxic conditions

Sorted CD271$^+$/CD146$^{-/low}$ and CD271$^+$/CD146$^+$ cells were plated on chamber slides and cultured for 6 days at 21% O_2. Cells that initially were CD146$^{-/low}$ continued to express CD146 at lower levels compared with CD146$^+$ cells (Figure 7A-B). Conversely, CD271 expression was comparable (Figure 7A-B). The difference in CD146 expression could also be observed flow cytometrically when analyzing lower-passage cultures generated from either CD146$^{-/low}$ or CD146$^+$ cells. However, the CD146 expression of CD271$^+$/CD146$^{-/low}$ cells progressively increased over time and attained levels comparable to those observed in cultured CD271$^+$/CD146$^+$ cells or cultures generated from unfractionated bone marrow by the end of the second passage (Figure 7C).

Because the expression levels of CD146 increased in normoxic culture and was related to the in situ localization of primary CFU-Fs, we examined the influence of oxygen levels on CD146 expression. Established stromal cultures from unsorted bone marrow (third and fourth passage) were cultured with or without deferoxamine mesylate (DFO) (n = 2). FACS analysis on day 7 showed that approximately 25% of the DFO-treated cells had become negative for CD146, compared with approximately 3.5% in untreated controls (Figure 7D). No changes in CD90 and CD271 expression were observed (supplemental Figure 6A). This finding was confirmed in hypoxic chamber experiments (n = 2), which showed that CD146 expression decreased after 2 weeks of culture in 1% O_2 compared with 21% O_2 (Figure 7E). This hypoxia-induced decrease of CD146 expression was reversible when cells were incubated for an additional 2 weeks at 21% O_2 (Figure 7E). No changes in expression levels could be detected for any of the remaining surface markers investigated (CD105, CD73, CD90, HLA class I, and CD271; supplemental Figure 6B).

Discussion

Nonhematopoietic BM-MSCs are capable of generating tissues such as bone, fat, and cartilage. Furthermore, BM-MSCs also give rise to the HME, which provides a niche for HSCs in vivo and plays a pivotal role in regulating, supporting, and maintaining hematopoiesis.[3,19,20]

Considerable progress has been made regarding the phenotypic description of BM-MSCs, and several surface markers for an effective enrichment of CFU-Fs have been reported. Nonetheless, a comprehensive characterization of the nonhematopoietic stem cell system and its different subpopulations is just beginning to emerge. Furthermore, relatively little is known about BM-MSCs and their role in the HME.

Recently, Sacchetti et al[3] identified a population of CD146$^+$ subendothelial human bone marrow cells that contained all assayable CFU-Fs and generated bone and HME when transplanted subcutaneously into immunodeficient mice. CD271 is another broadly accepted marker for CFU-Fs,[6,7] which stains a population of subendothelial and bone-lining stromal cells in human bone marrow.[21] We show herein by costaining of CD146 and CD271 that all assayable CFU-Fs were highly and exclusively enriched, not only in the CD146$^+$ fraction of lin$^-$/CD271$^+$/CD45$^-$ stem cells, but also in the CD146$^{-/low}$ fraction, thus complementing the current knowledge.

Whereas Sacchetti et al used CD146$^+$ and CD146$^-$ FACS sorting of MACS CD45-depleted BM-MNCs, we started with a

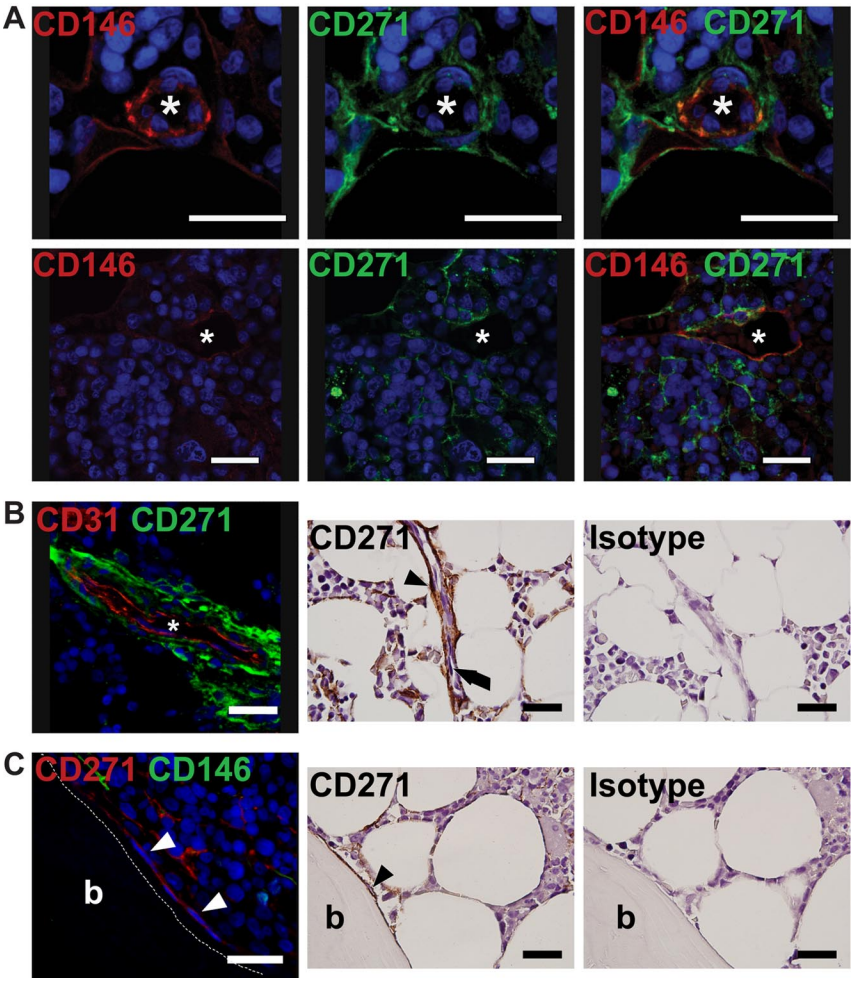

Figure 5. In situ localization of CD271 and CD146 bone marrow cells. Immunofluorescence staining for the in situ localization of primary BM-MSCs. Paraffin sections of normal human bone marrow biopsies were stained with antibodies against CD271 and CD146. (A) Double-positive cells were detected as reticular cells surrounding the endothelium of vessels. Photographs in the left and middle panels illustrate staining against one antigen in double-stained specimens; these photographs are merged in the right panel. (B) CD271$^+$ reticular cells, shown as green cells in the left panel and brown cells (black arrowhead) in the immunohistochemical (IHC) panels, were found as perivascular cells surrounding the endothelium, shown as red CD31$^+$ cells in the left panel and black arrow in the middle IHC panel. (C) CD271$^+$ bone-lining cells (white arrowheads in the left panel and black arrowhead in the IHC photograph) showed no expression of CD146 (green in the left panel). (B-C) Right IHC panels show a control for the CD271 staining using an isotype-matched antibody. IHC photographs were counterstained with hematoxylin. For confirming IHC expression analysis of CD146 on bone-lining CD271$^+$ cells, see supplemental Figure 5. Nuclei were stained with TO-PRO3 (blue). Scale bars indicate 25 μm. Asterisk indicates the lumen of a vessel. Trabecular bone (b) is indicated. Immunofluorescence photographs were taken with a confocal microscope (DMRE; Leica); IHC photographs were taken with an upright microscope (BX51; Olympus).

highly enriched population of lin$^-$/CD45$^-$/CD271$^+$ cells for sorting on CD146 expression, which is the likely reason that the very rare population of CD146$^{-/low}$ CFU-Fs became assayable in our experiments.

In agreement with previous studies, the majority of CD271$^+$ cells coexpressed CD45$^+$.[22] Therefore, even though CD271—in contrast to CD146—identified all human BM-CFU-Fs, it is necessary to also exclude CD45$^+$ hematopoietic cells from the population to reach a high purity of BM-CFU-Fs.

In addition to differences in CD146 expression, both CD271$^+$ populations showed comparable BM-MSC properties (morphology, surface-marker expression, in vitro and in vivo differentiation capacities, stroma-supporting capacities, and secondary colony formation). However, differences in CD146 expression were

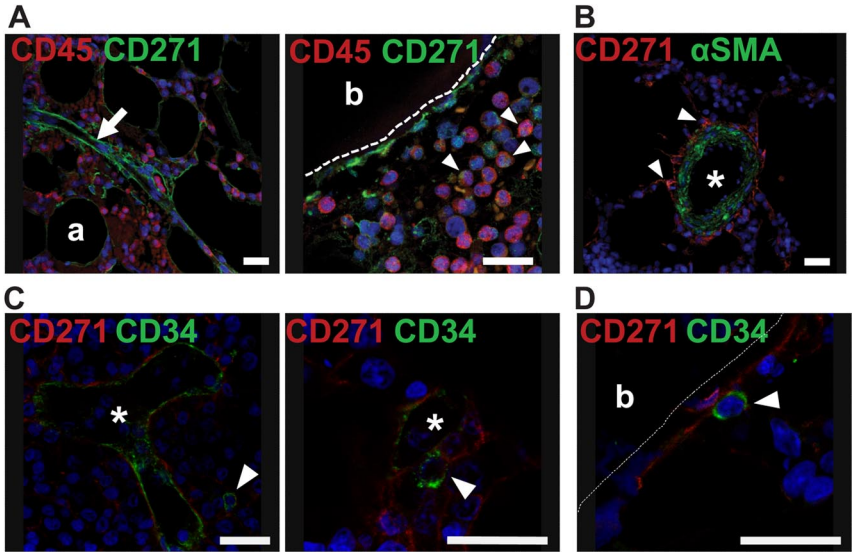

Figure 6. CD45 and α-SMA expression on BM-CFU-Fs and colocalization of BM-CFU-Fs with CD34$^+$ cells. (A) Human bone marrow paraffin sections were stained with antibodies against CD271 and CD45. White arrow indicates a vessel with perivascular CD271$^+$/CD45$^-$ cells (left). White arrowheads indicate round, hematopoietic CD271^{low}/CD45$^+$ cells (right). Bone-lining cells in the right photograph are CD271$^+$/CD45$^-$. (B) A larger vessel costained with CD271 and α-SMA is shown. White arrowheads indicate CD271$^+$/α-SMA^{low} perivascular cells. (C-D) Bone marrow sections were stained against CD34 to detect hematopoietic stem/progenitor cells and against CD271 to detect CFU-Fs. (C) Round CD34$^+$ cells (green) were found in proximity to the reticular extensions of perivascular CD271$^+$ cells (red). (D) In rare instances, round CD34$^+$ cells (green) were found neighboring CD271$^+$ cells in endosteal regions. White arrowheads indicate CD34$^+$ cells. Nuclei were stained with TO-PRO3 (blue). Scale bars indicate 25 μm. Asterisks indicate the lumen of a vessel. Trabecular bone (b) is indicated. Photographs were taken with a confocal microscope (DMRE; Leica). For the expression of α-SMA and perivascular localization of CD271$^+$ cells, see supplemental Figure 5.

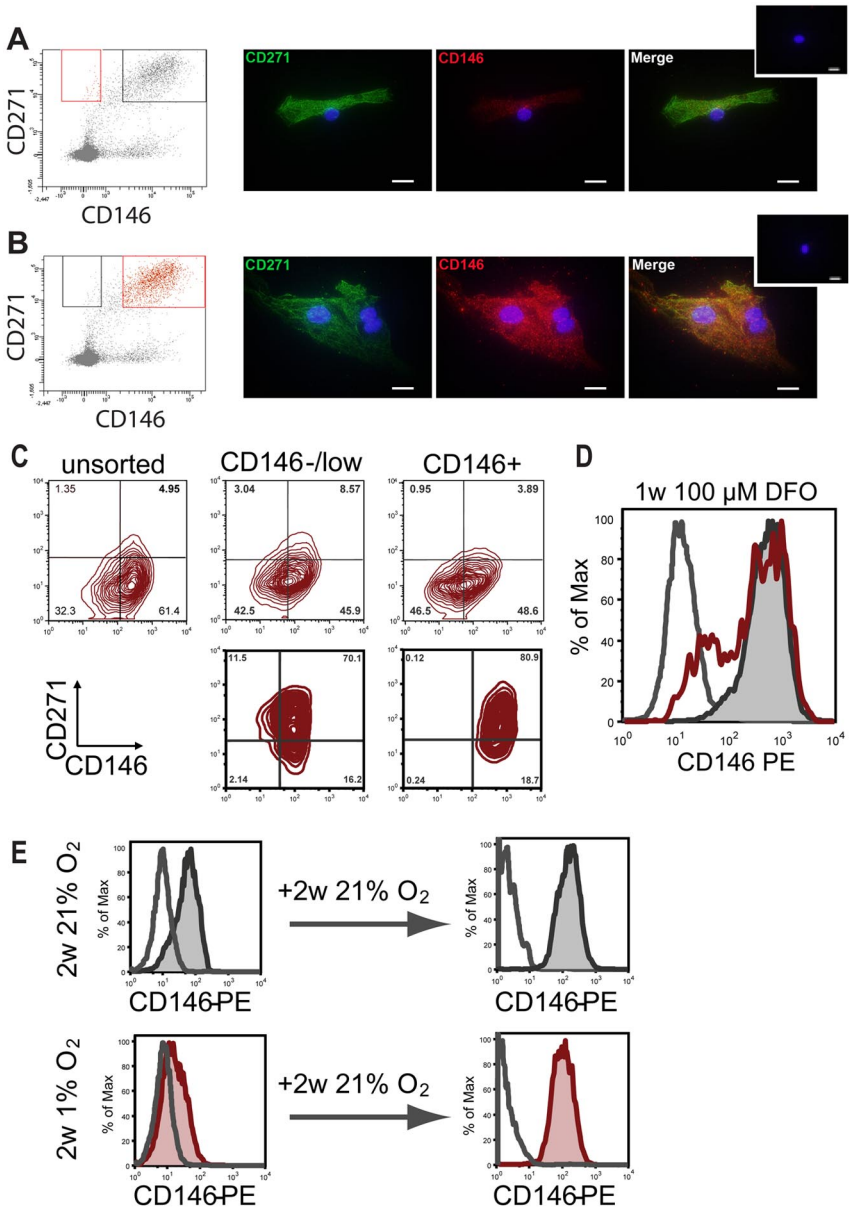

Figure 7. In vitro CD146 expression under normoxic and hypoxic conditions. CD146 expression of CD271$^+$/CD45$^-$/CD146$^{-/low}$ and CD271$^+$/CD45$^-$/CD146$^+$ cells was monitored over time. Sorted cells from the CD146$^{-/low}$ (A) and the CD146$^+$ (B) fractions were plated on glass chamber slides. Original sorting gates are shown in red on the left. Cells were incubated at 37°C, 5% CO_2, and 21% O_2. On day 6, cells were stained with antibodies against CD271 (green) and CD146 (red) plus the corresponding secondary antibodies. Small inserted photographs on the top right show controls stained with secondary antibodies only. Scale bars indicate 20 μm. (C) CD146 and CD271 expression in cultured cells after the second passage. Stromal cultures were generated from unsorted BM-MNCs (top left), bulk-sorted CD271$^+$/CD45$^-$/CD146$^{-/low}$ cells (top middle), or CD271$^+$/CD45$^-$/CD146$^+$ cells (top right). FACS plots in the bottom row show CD146 and CD271 expression of clonal second-passage cultures from a CD271$^+$/CD45$^-$/CD146$^{-/low}$–sorted cell (bottom left) and a CD271$^+$/CD45$^-$/CD146$^+$ sorted cell (bottom right), respectively. (D) Representative FACS histogram plot of cells cultured for 1 week with 100μM DFO (red open histogram). Controls were cultured without DFO (gray tinted histogram). Gray open histogram indicates isotype control. (E) Representative FACS plots for CD146 expression of established stromal cells cultured at 21% O_2 (gray tinted histogram, top left) or at 1% O_2 (red tinted histogram, bottom left). Increased expression and reexpression of CD146, respectively, was observed when both normoxic and hypoxic stromal cells were passaged and both were incubated for an additional 2 weeks at 21% O_2 (gray and red tinted histograms in right top and bottom row, respectively). Open histograms represent isotype controls.

clearly correlated with in situ localization, and therefore enabled us to identify endosteally localized CD271$^+$/CD146$^{-/low}$ cells and perivascular CD271$^+$/CD146$^+$ cells. These observations agree with the findings by Sacchetti et al[3] on the localization of bone marrow CD146$^+$ adventitial reticular cells and with data by Cattoretti et al[21] reporting that CD271$^+$ stromal cells can be found as either perivascular or bone-lining cells.

As a note of caution, it has not been ultimately proven at present whether all of the CD271$^+$/CD45$^-$/CD146$^{-/low}$ and CD271$^+$/CD45$^-$/CD146$^+$ cells that we identified in situ represent CFU-Fs, because some of the cells could belong to the fraction of non-colony-forming cells that might still be present even in highly purified cell populations (here, an even more precise BM-MSCs phenotype definition would be necessary). From our coexpression analysis, CD105, CD90, CD49a, PDGFR-β, and Stro-1 appear to be potentially useful as additional CFU-F marker candidates. However, in contrast to what has been reported previously, we did not observe expression of SSEA-4 and GD2 on primary BM-MSCs, which might have been due to differences in staining and analysis protocols.

In bone marrow sections, both CD271$^+$/CD146$^{-/low}$ and CD271$^+$/CD146$^+$ cells were associated with CD34$^+$ hematopoietic cells, and to our knowledge this is the first report demonstrating the association of distinct BM-MSC subsets with different potential HSC niche cell types in the human system. These observations agree with recently published landmark findings showing that nestin-positive mesenchymal stem cells form a niche for HSCs in murine bone marrow.[23] In that study, murine nestin$^+$/CD45$^-$ cells were identified as a small population of quiescent, perivascular BM-MNCs, which could differentiate into multiple skeletal lineages, possessed self-renewal capacity, and were required for HSC homing and maintenance of HSC. Interestingly, the genome-wide expression profile of these cells was closest to that of human CD146$^+$ BM-MSCs.[23] In comparison, the human multipotent CD271$^+$/CD45$^-$ BM-MSCs described herein also showed nestin expression and exhibited hematopoietic stroma characteristics in

vitro and in vivo. The total population of $CD271^+/CD45^-$ cells in human BM-MNCs identified in our study was somewhat smaller (0.03%) than the reported nonhematopoietic nestin-positive population (0.08%) in mouse bone marrow; however, CFU-F frequency in the human $CD271^+/CD45^-$ population was higher (approximately 10-fold) compared with the murine cells.

It has been suggested that different endosteal and perivascular HSC niche cell types exist, and that different hematopoietic subsets reside in distinct localizations of the murine bone marrow[12-15,24-27]; for example, murine long-term HSCs reside in close proximity to the endosteal surface of trabecular bone.[26] Whether distinct human $CD34^+$ hematopoietic stem- and progenitor-cell populations colocalize with different localizations and the different BM-MSC populations as identified herein is certainly of great interest and will therefore be addressed in future experiments.

The concept that separate endosteal and perivascular stem cell niches exist in the bone marrow has been debated. Areas of trabecular bone are highly vascularized, and therefore endosteally located HSCs are most likely not only influenced by osteoblastic signaling, but also by vascular cells.[26,27] According to the findings in murine marrow, we observed a dense vasculature network in the human bone marrow biopsies studied, with vessels also located near the surface of trabecular bone. Nevertheless, it has been clearly demonstrated that an oxygen gradient exists in the bone marrow and that HSCs are localized at the lowest end of the gradient in hypoxic niches[28-32] such as the bone surface area.[28] We also observed that in vitro CD146 expression was dependent on oxygen levels and that in situ CD146 expression near the bone surface was absent or very weak. These observations might partly be explained by lower oxygen levels at the endosteum; however, additional mechanisms such as calcium-induced CD146 shedding might be operative as well,[33] because calcium levels are high near activated osteoclasts at the endosteal surface.[34]

In summary, we have defined the phenotype of human primary nonhematopoietic BM-MSCs based on the expression of CD271, CD45, and CD146. We demonstrate that CD146 expression in lineage-negative, NGFR-positive, common leukocyte antigen–negative stroma stem cells is correlated with in situ localization, and that different BM-MSC subpopulations colocalize with different putative HSC niche cell types. This is an important finding that is likely to be the first step toward a better characterization of the human HME, hopefully leading to a better understanding of niche anatomy and function in normal and diseased marrow.

Acknowledgments

We thank Håkan Axelson and Olle Lindvall for their help and support with the hypoxic chamber experiments and confocal microscopy, respectively, and Marja Ekblom for critical discussions and helpful suggestions.

This work was supported by funds from the Swedish Research Council (VR), the Crafoord Foundation, the Swedish Childhood Cancer Foundation, Gunnar Nilsson's Cancer Foundation, the Lundgren Foundation, John Persson's Foundation, ALF (Government Public Health Grant), and the Skane County Council's Research and Development Foundation. The Lund Stem Cell Center is supported by a Center of Excellence Grant from the Swedish Foundation for Strategic Research.

Authorship

Contribution: A.T. performed and designed research, analyzed and interpreted data, and wrote the manuscript; O.L., J.C.B., S.W., B.S., and N.D. performed research and analyzed and interpreted data; M.E. contributed vital samples and analyzed and interpreted data; M.K. analyzed and interpreted data; and S.S. designed research, analyzed and interpreted data, and wrote the manuscript.

Conflict-of-interest disclosure: The authors declare no competing financial interests.

Correspondence: Stefan Scheding, MD, Lund Stem Cell Center, University of Lund, BMC B10, Klinikgatan 26, 22184 Lund, Sweden; e-mail: stefan.scheding@med.lu.se.

References

1. Ashton BA, Allen TD, Howlett CR, et al. Formation of bone and cartilage by marrow stromal cells in diffusion chambers in vivo. *Clin Orthop Relat Res.* 1980;(151):294-307.
2. Krebsbach PH, Kuznetsov SA, Satomura K, et al. Bone formation in vivo: comparison of osteogenesis by transplanted mouse and human marrow stromal fibroblasts. *Transplantation.* 1997;63(8):1059-1069.
3. Sacchetti B, Funari A, Michienzi S, et al. Self-renewing osteoprogenitors in bone marrow sinusoids can organize a hematopoietic microenvironment. *Cell.* 2007;131(2):324-336.
4. Bianco P, Robey PG, Simmons PJ. Mesenchymal stem cells: revisiting history, concepts, and assays. *Cell Stem Cell.* 2008;2(4):313-319.
5. Gronthos S, Graves SE, Ohta S, Simmons PJ. The STRO-1+ fraction of adult human bone marrow contains the osteogenic precursors. *Blood.* 1994;84(12):4164-4173.
6. Jones EA, Kinsey SE, English A, et al. Isolation and characterization of bone marrow multipotential mesenchymal progenitor cells. *Arthritis Rheum.* 2002;46(12):3349-3360.
7. Quirici N, Soligo D, Bossolasco P, et al. Isolation of bone marrow mesenchymal stem cells by anti-nerve growth factor receptor antibodies. *Exp Hematol.* 2002;30(7):783-791.
8. Gang EJ, Bosnakovski D, Figueiredo CA, Visser JW, Perlingeiro RC. SSEA-4 identifies mesenchymal stem cells from bone marrow. *Blood.* 2007;109(4):1743-1751.
9. Martinez C, Hofmann TJ, Marino R, Dominici M, Horwitz EM. Human bone marrow mesenchymal stromal cells express the neural ganglioside GD2: a novel surface marker for the identification of MSCs. *Blood.* 2007;109(10):4245-4248.
10. Deschaseaux F, Gindraux F, Saadi R, et al. Direct selection of human bone marrow mesenchymal stem cells using an anti-CD49a antibody reveals their CD45med, low phenotype. *Br J Haematol.* 2003;122(3):506-517.
11. Sorrentino A, Ferracin M, Castelli G, et al. Isolation and characterization of CD146+ multipotent mesenchymal stromal cells. *Exp Hematol.* 2008;36(8):1035-1046.
12. Zhang J, Niu C, Ye L, et al. Identification of the haematopoietic stem cell niche and control of the niche size. *Nature.* 2003;425(6960):836-841.
13. Calvi LM, Adams GB, Weibrecht KW, et al. Osteoblastic cells regulate the haematopoietic stem cell niche. *Nature.* 2003;425(6960):841-846.
14. Arai F, Hirao A, Ohmura M, et al. Tie2/angiopoietin-1 signaling regulates hematopoietic stem cell quiescence in the bone marrow niche. *Cell.* 2004;118(2):149-161.
15. Sugiyama T, Kohara H, Noda M, Nagasawa T. Maintenance of the hematopoietic stem cell pool by CXCL12-CXCR4 chemokine signaling in bone marrow stromal cell niches. *Immunity.* 2006;25(6):977-988.
16. Ahrens N, Tormin A, Paulus M, et al. Mesenchymal stem cell content of human vertebral bone marrow. *Transplantation.* 2004;78(6):925-929.
17. Tormin A, Brune JC, Olsson E, et al. Characterization of bone marrow-derived mesenchymal stromal cells (MSCs) based on gene expression profiling of functionally defined MSCs subsets. *Cytotherapy.* 2009;11(2):114-128.
18. Abdallah BM, Ditzel N, Kassem M. Assessment of bone formation capacity using in vivo transplantation assays: procedure and tissue analysis. *Methods Mol Biol.* 2008;455:89-100.
19. Adams GB, Scadden DT. The hematopoietic stem cell in its place. *Nat Immunol.* 2006;7(4):333-337.
20. Kiel MJ, Morrison SJ. Uncertainty in the niches that maintain haematopoietic stem cells. *Nat Rev Immunol.* 2008;8(4):290-301.
21. Cattoretti G, Schiro R, Orazi A, Soligo D, Colombo MP. Bone marrow stroma in humans: anti-nerve growth factor receptor antibodies selectively stain reticular cells in vivo and in vitro. *Blood.* 1993;81(7):1726-1738.
22. Poloni A, Maurizi G, Rosini V, et al. Selection of CD271(+) cells and human AB serum allows a large expansion of mesenchymal stromal cells

from human bone marrow. *Cytotherapy.* 2009; 11(2):153-162.

23. Méndez-Ferrer S, Michurina TV, Ferraro F, et al. Mesenchymal and haematopoietic stem cells form a unique bone marrow niche. *Nature.* 2010; 466(7308):829-834.
24. Heissig B, Hattori K, Dias S, et al. Recruitment of stem and progenitor cells from the bone marrow niche requires MMP-9 mediated release of kit-ligand. *Cell.* 2002;109(5):625-637.
25. Wilson A, Trumpp A. Hematopoietic stem cell niches. In: Wickrema A, Kee B, eds. *Molecular Basis of Hematopoiesis*. New York: Springer; 2009:47-71.
26. Lo Celso C, Fleming HE, Wu JW, et al. Live-animal tracking of individual haematopoietic stem/progenitor cells in their niche. *Nature.* 2009; 457(7225):92-96.
27. Xie Y, Yin T, Wiegraebe W, et al. Detection of functional haematopoietic stem cell niche using real-time imaging. *Nature.* 2009;457(7225):97-101.
28. Lévesque JP, Winkler IG, Hendy J, et al. Hematopoietic progenitor cell mobilization results in hypoxia with increased hypoxia-inducible transcription factor-1 alpha and vascular endothelial growth factor A in bone marrow. *Stem Cells.* 2007;25(8):1954-1965.
29. Simsek T, Kocabas F, Zheng J, et al. The distinct metabolic profile of hematopoietic stem cells reflects their location in a hypoxic niche. *Cell Stem Cell.* 2010;7(3):380-390.
30. Jang YY, Sharkis SJ. A low level of reactive oxygen species selects for primitive hematopoietic stem cells that may reside in the low-oxygenic niche. *Blood.* 2007;110(8):3056-3063.
31. Parmar K, Mauch P, Vergilio JA, Sackstein R, Down JD. Distribution of hematopoietic stem cells in the bone marrow according to regional hypoxia. *Proc Natl Acad Sci U S A.* 2007;104(13): 5431-5436.
32. Winkler IG, Barbier V, Wadley R, Zannettino AC, Williams S, Levesque JP. Positioning of bone marrow hematopoietic and stromal cells relative to blood flow in vivo: serially reconstituting hematopoietic stem cells reside in distinct nonperfused niches. *Blood.* 2010;116(3):375-385.
33. Boneberg EM, Illges H, Legler DF, Furstenberger G. Soluble CD146 is generated by ectodomain shedding of membrane CD146 in a calcium-induced, matrix metalloprotease-dependent process. *Microvasc Res.* 2009;78(3):325-331.
34. Silver IA, Murrills RJ, Etherington DJ. Microelectrode studies on the acid microenvironment beneath adherent macrophages and osteoclasts. *Exp Cell Res.* 1988;175(2):266-276.